Inorganic Chemistry

Article

pubs.acs.org/IC

Steady-State and Time-Resolved Investigations on Pyrene-Based Chemosensors

Javier Fernández-Lodeiro,[†,‡] Cristina Núñez,[‡] Catherine S. de Castro,[§] Emilia Bértolo,[⊥] J. Sérgio Seixas de Melo,*[,§] José Luis Capelo,[†,‡] and Carlos Lodeiro*[,†,‡]

[†]Grupo BIOSCOPE, Departamento de Química, Facultade de Ciencias, Campus de Ourense, Universidade de Vigo, 32004 Vigo, Spain

[‡]REQUIMTE/CQFB, Departamento de Química, Faculdade de Ciências e Tecnologia, Universidade Nova de Lisboa, 2829-516 Monte de Caparica, Portugal

[§]Department of Chemistry, University of Coimbra, 3004-535 Coimbra, Portugal

[⊥]Ecology Research Group, Department of Geographical and Life Sciences, Canterbury Christ Church University, Canterbury, Kent CT1 1QU, United Kingdom

Supporting Information

ABSTRACT: Two novel fluorescent probes bearing a single (**P**) and two (a podand-like structure, **L**) pyrene units derived from 1,5-bis(2-aminophenoxy)-3-oxopentane have been synthesized and investigated in dioxane using UV−vis absorption, and steady-state and time-resolved (in a picosecond time scale) emission spectroscopy; in the gas phase, matrix-assisted laser desorption ionization mass spectrometry was employed. In dioxane, the absorption and emission spectra of **P** present a unique band with maxima at 361 and 392 nm, which have been associated with the monomer absorption and emission bands, respectively. In dioxane, for compound **L**, an additional band with a maximum at ∼525 nm is observed; upon the addition of water, an emissive band (with maxima varying from 405 to 490 nm) appears in both **P** and **L** spectra; this is discussed in terms of the emission of a species with charge character. Upon metal addition (Cu^{2+}, Zn^{2+}, and Ag^{+}) to **P**, a gradual quenching effect of the monomer emission is observed and found to be more pronounced with Cu^{2+}. In the case of **L**, upon the addition of metal cations, the long emission band (∼550 nm) decreases and the monomer emission band increases (with an isoemissive point at ∼450 nm) and no evidence for the intermediate band (at ∼405−490 nm) now exists. Time-resolved data in dioxane/water mixtures showed that for **P** and **L** these two fit double- and triple-exponential decay laws, respectively. With **P**, this has been attributed to a two-state system, which involves the monomer and a charged species, with its emission maxima varying with the polarity of the media (here mirrored by its dielectric constant), which can potentially be addressed to an exciplex-like species, whereas with **L**, it has been attributed to a three-state system involving, in addition to these two species, an excimer. From absorption and fluorescence excitation and time-resolved data, evidence is given for the presence of intramolecular dimer formation in the ground state.

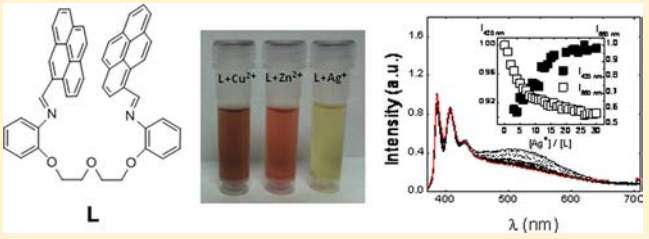

INTRODUCTION

Selective detection of transition-metal ions using self-organized Schiff-base host molecules is an area of considerable interest in the field of supramolecular chemistry.[1,2] Several conjugate macrocyclic and acyclic Schiff-base chemosensors based on polyoxa and/or oxaaza,[3] polyaza,[4] and azathia[5] receptor units have been reported. Our research group has studied a number of polyaza, polyoxaaza, and polythioaza systems as potential chemosensors for the recognition of metal ions.[6]

The synthesis of highly sensitive and selective chemosensors that can detect heavy- and transition-metal ions such as Hg^{2+}, Pb^{2+}, Cd^{2+}, and Cu^{2+} is attracting considerable attention.[7] One possible way of detecting cations is by using fluorescence spectroscopy as the sensing tool of choice; fluorescence spectroscopy is a very sensitive technique and is inexpensive, versatile, and nondestructive, and the experiments are easily performed.[8] Chemosensors based on the ion-induced changes in fluorescence have been actively investigated because of their simplicity and high detection limit.[9] The sensing ability of a fluorescence chemosensor is dependent upon the interaction between the ionophore (the recognizing unit responsible for selectively binding the ions) and the fluorophore (the fluorogenic unit for signal transduction) by either enhancement or inhibition of the fluorescence signal.[10] Signal-conducting mechanisms such as photoinduced electron transfer, intramolecular charge transfer, and Förster resonance energy transfer provide the connection between the binding event and reported signal.[11]

Received: June 26, 2012
Published: December 11, 2012

   dx.doi.org/10.1021/ic301365y | *Inorg. Chem.* 2013, 52, 121−129

Scheme 1. Synthesis of Molecular Probes P and L

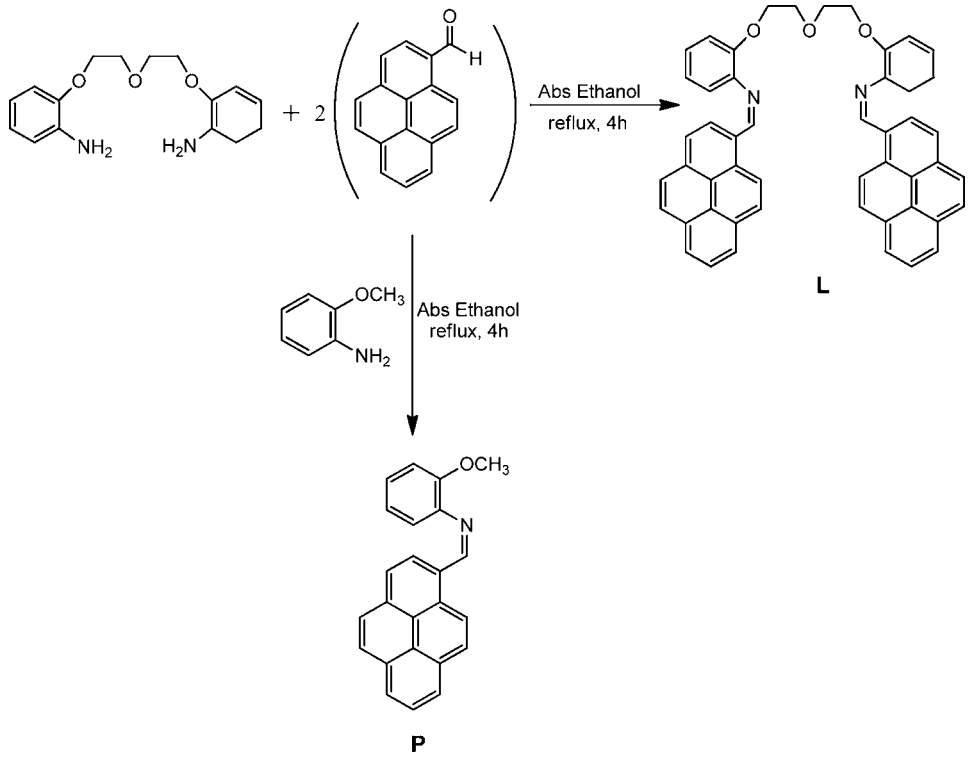

The pyrene moiety is one of the most useful fluorophores for the construction of fluorescence chemosensors.[12] Two pyrene moieties situated close enough can yield face-to-face interaction, which can be sandwich-like or deviated from the planarity orientation for the excimer emission.[13] Moreover, the intramolecular interaction of the pyrene units can be made in the ground (dimer) or excited state, leading to changes in the spectra (absorption, emission, and excitation) and photophysical behavior. The presence of the absorption of an intramolecular dimer will also lead to a contribution of direct excitation of this species to the long emission band characteristic of the pyrene excimer. Indeed, upon coordination with a specific guest ion, the resulting compound could be fine-tuned to yield monomer and/or excimer/dimer emissions depending on the orientation of the two pyrene moieties.[14] On the basis of the pyrene ratio of monomer versus excimer emission, several "on−off" recognition systems for heavy- and transition-metal ions have been successfully devised.[15]

In this work, we report the synthesis and photophysical characterization of two new fluorescence probes, **P** and **L**. Chemosensor **L** contains two emissive pyrene units as chromophores, linked by a flexible polyoxaethylene bridge and chemosensor **P** a single pyrene unit.

EXPERIMENTAL SECTION

Physical Measurements. Elemental analyses were performed in a Fisons EA-1108 analyzer at the CACTI, University of Vigo Elemental Analyses Service. IR spectra were recorded as KBr disks on a Bio-Rad FTS 175-C spectrophotometer. ^{1}H, ^{13}C, COSY, DEPT, and HMQC NMR spectra were recorded on a Bruker AMX-500 spectrometer, and dimethyl sulfoxide (DMSO) was used as the solvent in all cases.

Matrix-assisted laser desorption ionization time-of-flight mass spectrometry (MALDI-TOF-MS) analysis was performed in a MALDI-TOF-MS model Bruker Ultraflex II workstation equipped with a nitrogen laser radiating at 337 nm from Bruker (Germany) at the BIOSCOPE Group. The spectra represent accumulations of 5 × 100 laser shots. The reflectron mode was used. The ion source and flight tube pressures were less than 1.80×10^{-7} and 5.60×10^{-7} Torr, respectively. The MALDI-MS spectra of the soluble samples (1 or 2 mg/mL), such as the ligand and metal complexes, were recorded using the conventional sample preparation method for MALDI-MS.

Chemicals and Starting Materials. 1,5-Bis(2-aminophenoxy)-3-oxopentane was synthesized following the method previously published;[20] 1-pyrenecarboxaldehyde and hydrated tetrafluoroborate metal salts were commercial products from Alfa and Aldrich and were used without further purifications.

Spectrophotometric and Spectrofluorimetric Measurements. UV−vis absorption spectra were performed using a Jasco 650 or a Shimadzu 2450 UV−vis spectrophotometer; fluorescence spectra were recorded on a Horiba Jobin-Yvon Fluoromax 4 spectrometer. All of the fluorescence spectra were corrected for the wavelength response of the system. The linearity of the fluorescence emission versus concentration was checked in the concentration range used (10^{-5}−10^{-6} M). A correction for the absorbed light was performed when necessary. The fluorescence decays of the compounds were obtained with picosecond resolution with equipment described elsewhere[17] and were analyzed using the method of modulating functions implemented by Striker et al.[18] The experimental excitation pulse [full width at half-height (fwhm) = 21 ps] was measured using a LUDOX scattering solution in water. After deconvolution of the experimental signal, the time resolution of the apparatus was ca. 2 ps.

All spectrofluorimetric titrations were performed as follows: a stock solution of the ligand was prepared by dissolving an appropriate amount of the ligand in dioxane and diluted to the desired concentration ([**P**] = [**L**] = 5.00×10^{-6} M). Titrations were carried out by the addition of microliter amounts of standard solutions of the ions dissolved in the same solvent. All of the measurements were performed at 298 K.

Synthesis of Organic Ligands. *Synthesis of P.* A solution of 2-methoxyaniline (0.124 g, 1.006 mmol) in absolute ethanol (20 mL) was added dropwise to a refluxing solution of 1-pyrenecarboxaldehyde (0.231 g, 1.006 mmol) in the same solvent (50 mL). The resulting

dx.doi.org/10.1021/ic301365y | *Inorg. Chem.* 2013, 52, 121−129

solution was gently refluxed with magnetic stirring for ca. 4 h. The yellow powder precipitate formed was filtered off, washed several times with cold absolute ethanol, dried under vacuum, and characterized as compound **P**. The compound was found to be soluble in acetonitrile, decane, dichloromethane, dioxane, DMSO, toluene, and water and insoluble in absolute ethanol, methanol, and diethyl ether.

Synthesis of L. A solution of 1,5-bis(2-aminophenoxy)-3-oxopentane (0.153 g, 0.531 mmol) in absolute ethanol (50 mL) was added dropwise to a refluxing solution of 1-pyrenecarboxaldehyde (0.247 g, 1.062 mmol) in the same solvent (75 mL). The resulting solution was gently refluxed with magnetic stirring for ca. 4 h. Solvent removal produced a red oil, which was washed three times with a mixture of cold cyclohexane/diethyl ether. A red powder precipitate formed and was filtered off and dried under vacuum. The compound was characterized as chemosensor **L**. Compound **L** was soluble in acetonitrile, decane, dichloromethane, dioxane, DMSO, toluene, and water and insoluble in absolute ethanol, methanol, and diethyl ether.

P. Anal. Calcd for $C_{24}H_{17}NO.H_2O$: C, 81.5; H, 5.4; N, 3.9. Found: C, 81.6; H, 5.4; N, 3.9. Yield: 89%. IR (KBr): 1649 [ν(C═N) $_{imine}$] cm^{-1}. MALDI-TOF-MS: m/z 336.21 ([**P** + H]$^+$). Color: yellow. ^{1}H NMR (400 MHz, DMSO): δ 8.87 (s, 1H), 8.46−6.68 (m, 9H), 3.85 (s, 3H).

L. Anal. Calcd for $C_{50}H_{38}N_2O_3{\cdot}H_2O$: C, 81.3; H, 5.5; N, 3.8. Found: C, 81.6; H, 5.7; N, 3.8. Yield: 81%. IR (KBr): 1647 [ν(C═N) $_{imine}$] cm^{-1}. MALDI-TOF-MS: m/z 713.11 ([**L** + H]$^+$). Color: red. ^{1}H NMR (400 MHz, DMSO): δ 9.58 (s, 2H), 8.71−7.98 (m, 18H), 7.32−6.21 (m, 8H), 4.26−4.00 (m, 2H), 3.92−3.77 (m, 2H).

RESULTS AND DISCUSSION

Synthesis. Probes **P** and **L** were synthesized, following a one-pot reaction, by direct condensation between the commercial carbonyl precursor 1-pyrenecarboxaldehyde and 2-methoxyaniline (**P**) or 1,5-bis(2-aminophenoxy)-3-oxopentane (**L**).[19] The final products **P** and **L** have been characterized by microanalysis, melting points, IR, ^{1}H and ^{13}C NMR, UV−vis and fluorescence emission spectroscopy, and MALDI-TOF-MS. All techniques confirm the integrity of these species in solution and in the gas phase (see the Supporting Information, SI). The reaction pathways for the synthesis of compounds **P** and **L** are shown in Scheme 1.

MALDI-TOF-MS Titrations. In order to explore the potential application of chemosensor **L** as a molecular probe for metal ions in the gas phase, several MALDI-TOF-MS titrations were performed. Compound **L** was dissolved in acetonitrile, without any additional external MALDI matrix. **L** was titrated with Ag^+, Cu^{2+}, Zn^{2+}, Cd^{2+}, and Hg^{2+} in 1:1 and 1:2 (ligand/metal) molar ratios. To perform the metal titrations, two different strategies were used, a dried droplet solution and a layer-by-layer deposition sample preparation. On the first method, two solutions containing compound **L** (1 μL) and the metal salt (1 μL) were first mixed and then applied in the MALDI-TOF-MS sample holder. On the second method, a solution of **L** was spotted in the MALDI-TOF-MS plate and then dried under vacuum; subsequently, 1 μL of the solution containing the metal salt was deposited on the sample holder and dried. The plate was then inserted into the ion source. On this second method, the complexation reaction between the ligand and metal salts occurred in the holder, and the complex species were produced directly in the gas phase.

The peak attributable to the protonated species [**L**H]$^+$ appears always at m/z 713.11. The titrations for Cu^{2+} and Ag^+ are shown in Figure 1. Irrespective of the sample preparation method, upon the addition of 1 equiv of Cu^{2+}, the peak attributable to the ligand disappears, and a new peak with 100% relative intensity appears at m/z 775.25, attributable

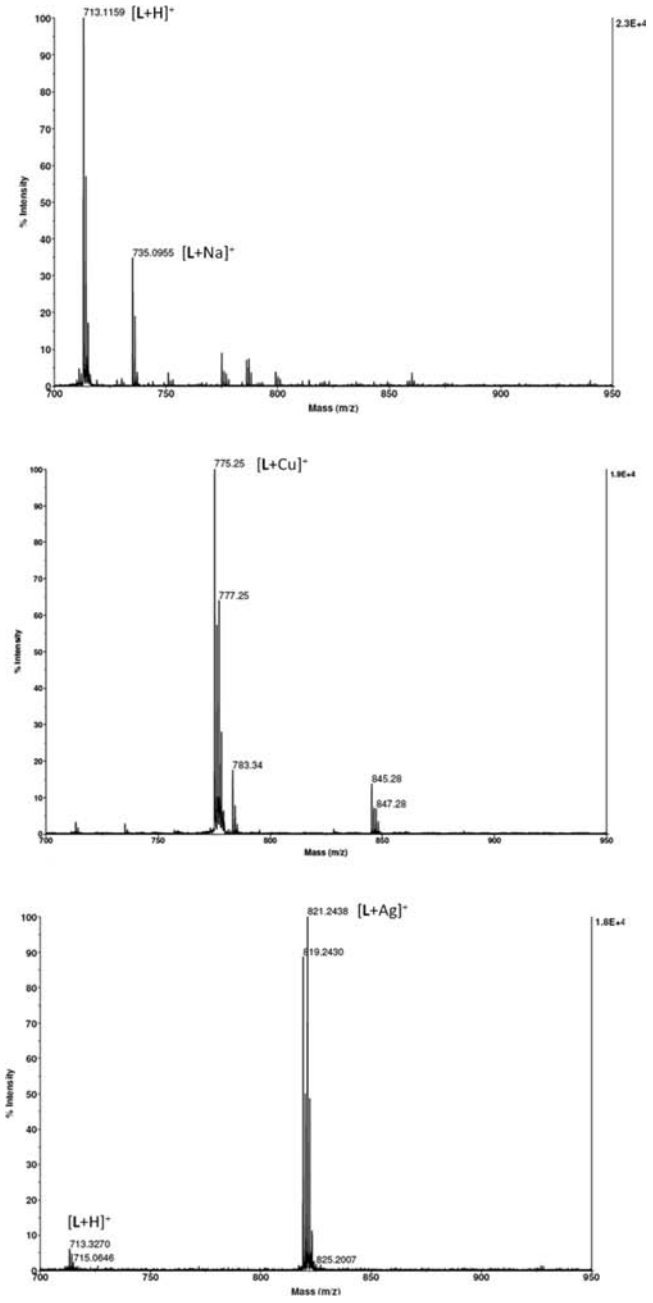

Figure 1. From top to bottom, MALDI-TOF-MS spectra of compound **L** before and after titration with $Cu(BF_4)_2{\cdot}6H_2O$ and $Ag(BF_4)_2$ (1 equiv of a metal ion). Note that the Na^+ ion on the top spectrum is from the glassware.

to the mononuclear species [**L**Cu]$^+$. In the titration with Ag^+, upon the addition of 1 equiv of Ag^+, an equivalent peak corresponding to the mononuclear species [**L**Ag]$^+$ appears at m/z 821.24 (100% relative intensity). No peaks attributable to dinuclear species were detected in either case. For Zn^{2+}, Cd^{2+}, and Hg^{2+}, the MALDI-TOF-MS titration did not show any peaks attributable to the metal complexes. These results suggest that **L** can be used to sense selectively Cu^{2+} and Ag^+ by MALDI-TOF-MS. Similar results were observed for an analogous system described previously.[20]

Spectrophotometric Studies. Absorption, emission, and excitation spectra of **P** and **L** were obtained in dioxane at 298 K, and the results are presented in Figure 2 and Table 1.

dx.doi.org/10.1021/ic301365y | *Inorg. Chem.* 2013, 52, 121−129

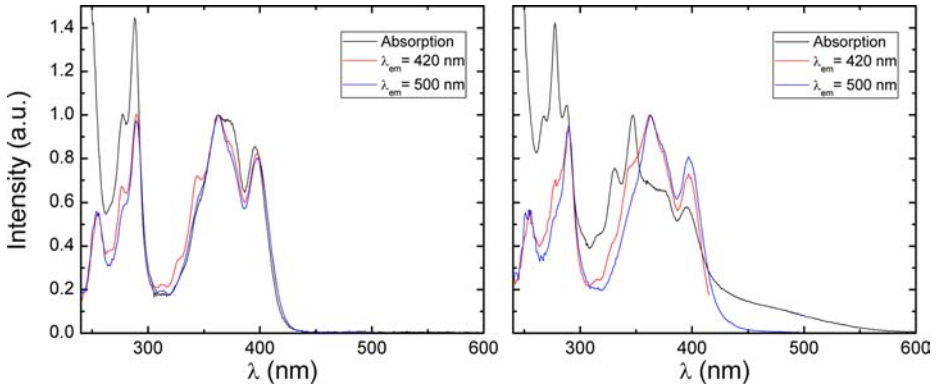

Figure 2. Absorption, emission, and excitation spectra of compounds **P** (left panel) and **L** (right panel) in dioxane. λ_{exc} = 360 nm, $\lambda_{em(P)}$ = 420 nm, $\lambda_{em1(L)}$ = 420 nm, $\lambda_{em2(L)}$ = 500 nm, and [**P**] = [**L**] = 5 × 10^{-6} M.

Table 1. Absorption, Emission, and Excitation Wavelength Maxima (λ_{max}^{A}, λ_{max}^{em}, and λ_{max}^{exc}) and Molar Extinction Coefficients (ε) for Chemosensors P and L in Dioxane at 298 K

compound	λ_{max}^{A} (nm)	log ε	λ_{max}^{em} (nm)	λ_{max}^{exc} (nm)*
P	361	4.65	392	361
L	348	4.74	386	349

*Obtained from the excitation spectra with emission collected at 420 nm (see Figure 2).

For **P**, both the absorption and emission spectra show a single band, which is attributed to the monomer (absorption and emission) of this compound by comparison with pyrene.[21] However, it should be noticed that in contrast with pyrene, where the first electronic transition has a forbidden character, in the case of **P**, the 0,0 transition is now allowed, as can be seen from Figure 2.

In the case of compound **L** in dioxane, an absorption band in the 400−500 nm region is now visible together with an emission band with maxima at ∼500 nm. Two potential reasons can be appointed to rationalize the origin of this band in **L**: (i) a small amount of water that persists from the synthetic and purification procedure, even if this is dried to exhaustion; (ii) the formation (resulting from the interaction between the two pyrene units in **L**) of an intramolecular dimer.

In dioxane, the presence of the 400−500 nm absorption band (seen as a tail) in **L** and its absence in **P** suggests that (ii) mirrors a more realistic situation. Along the text, the reference to this dimer should be viewed as resulting from an intramolecular interaction between the two pyrene units in **L**.

In the case of **L**, it is also worth noting that the excitation spectra collected in the monomer emission region mirrors the absorption spectra of the monomer (see Figure 2), whereas when collected in the long emission wavelength band (∼550 nm), it displays a band in 400−550 nm (Figure 2, right panel), which strongly suggests that the great majority of the latter

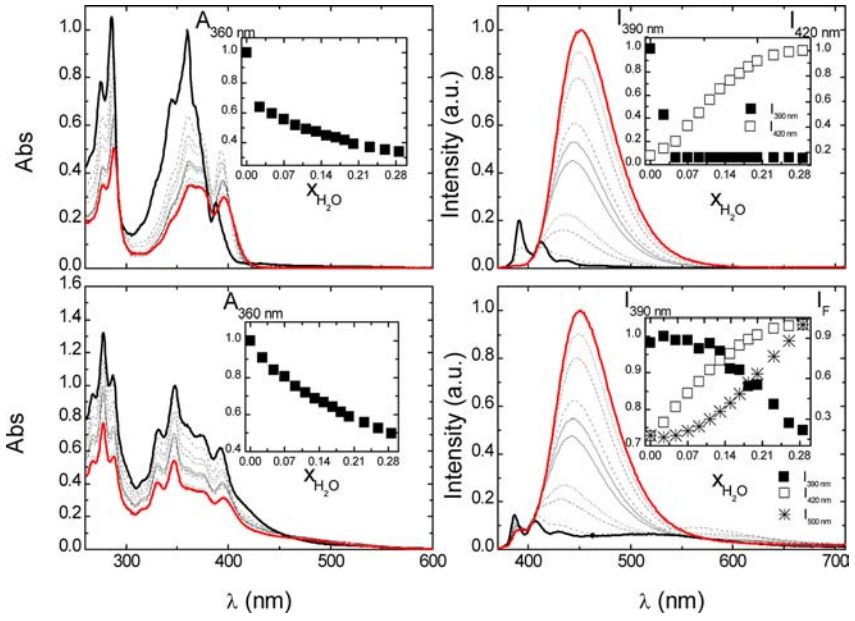

Figure 3. Absorption (left panels) and emission (right panels) spectra of **P** (top panels) and **L** (bottom panels) in dioxane at room temperature after the addition of water (λ_{exc} = 360 nm and [**P**] = [**L**] = 5.00 × 10^{-6} M). The insets show variation with the mole fraction of water of the absorption at 390 nm and the fluorescence intensities at 390 and 420 nm for **P** and 390, 420, and 500 nm for **L**. The bold dark line is for x_{H_2O} = 0, whereas the bold red line is for x_{H_2O} = 0.29.

dx.doi.org/10.1021/ic301365y | *Inorg. Chem.* 2013, 52, 121−129

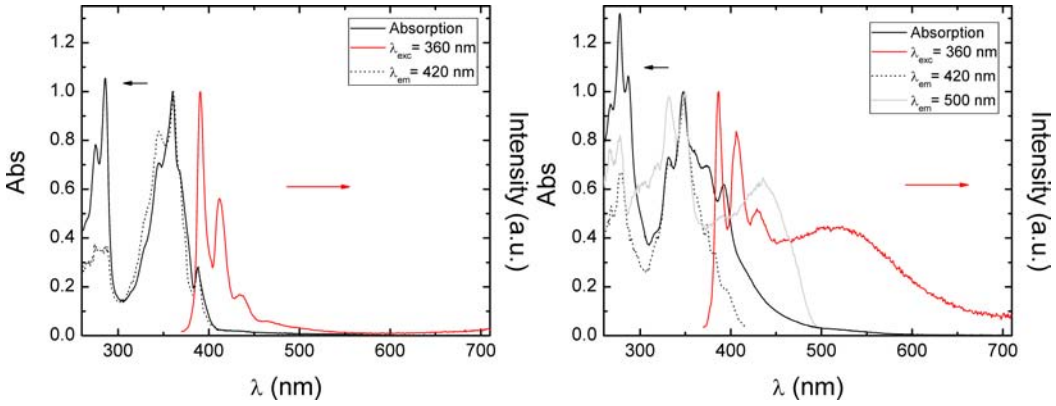

Figure 4. Absorption and fluorescence emission and excitation spectra (λ_{em1} = 420 nm for **P** and **L** and λ_{em2} = 500 nm for **L**) for **P** (left panel) and **L** (right panel) in a dioxane/water mixture with x_{H_2O} = 0.29.

band is originated through a static mechanism (from direct excitation of preformed intramolecular dimers).

P and L upon the Addition of Water. Upon the addition of water, a new band, in addition to the monomer (390 nm) band, appears for both **P** and **L** with a maximum that varies between 405 and 495 nm; see Figure 3.

By collection of the excitation spectra with emission in this band (i.e., at values in the extremities of this band: 420 and 500 nm), a vibronically resolved band with a maximum at 360 nm is observed for the two compounds (see Figure 4). This seems to attest further the identical nature of this band in the two compounds. Moreover, it is worth noticing the fact that with **P** upon collection at 420 and 500 nm, i.e., along this new band that only appears by the addition of water, the excitation spectra match the absorption spectra. The same is, however, not valid for **L**, where although the excitation bands when collected at 420 and 500 nm are identical, a partial departure from full overlap with the absorption spectra is now obtained. This suggests that in the case of **L** the long emission band is the result of more than one species; i.e., one is identical with that observed with **P** (not absorbing in the ground state, as attested by the left top panel in Figure 3), and the additional band (in **L**) is likely to be due to the excimer/dimer, which is also present in the ground state.

As can be seen from Figure 3, water strongly influences the absorption and emission spectra of **L**. To exclude the possibility of reaction between **L** and water, an independent experiment was carried out involving the run of the absorption spectra upon the (i) addition of water to **L** and (ii) subsequent removal of water from **L**. A solution of **L** in a dioxane/water mixture (x_{H_2O} = 0.80) was dried with the aim of complete removal of the solvent mixture (water included). The dried compound (in a film form) was again dissolved in dioxane; the two obtained spectra (before and after the removal of water) were found to be identical (Figure S4 in the SI).

In order to have further knowledge on the nature of the emissive species at long emission in both **P** and **L**, the emission wavelength maximum of this emission band was plotted as a function of the water fraction and dielectric constant[22] of the media for T = 293 K; see Figure 5. It can be seen that this band red-shifts with an incremental amount of water and that the values are basically identical with the two compounds in the same dioxane/water mixtures. The pronounced red shift of this band with the increase in the dielectric constant of the media strongly suggests the presence of a charged species. Others with

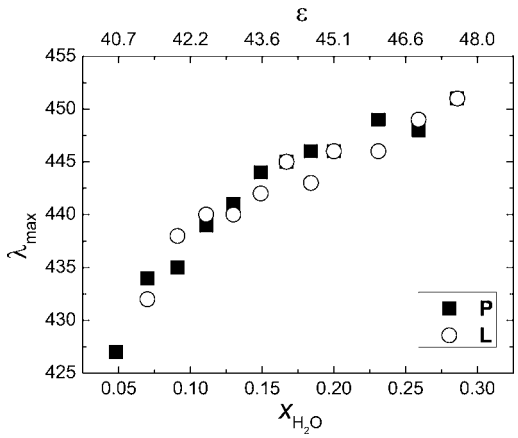

Figure 5. Dependence of the wavelength maxima (λ_{max}) with the mole fraction of water (x_{H_2O}) and the dielectric constant (ε) taken from the emission spectra of **P** (closed symbols) and **L** (open symbols) for λ_{exc} = 360 nm and [**P**] = [**L**] = 5 × 10^{-6} M.

similar compounds have associated the shift of this emergent band to an exciplex.[23] However, further and convincing arguments on the nature of this band come from time-resolved data (see below).

Time-Resolved Data for P and L in Dioxane/Water Mixtures. The fluorescence decays for the two compounds (**P** and **L**) were obtained with excitation at 381 nm (monomer absorption band; see Figure 2) and were collected at 420 and 500 nm for **P** and 420 and 550 nm for **L**. With both **P** and **L**, the longest emission wavelength was specifically chosen away from its maximum in order to avoid emission contribution from the monomer species. Upon the addition of water to **P**, the fluorescence decays are now biexponential (with values ranging from 40 to 70 ps and from 190 to 700 ps), whereas with **L**, these are only properly fit to a triexponential decay law; see Figure 6.

With **P**, the two decay times increase with the addition of water, but clearly the longer decay time increases deeply. Moreover, whereas at the monomer (420 nm) emission wavelength the preexponential factors are kept rather constant (ranging from 0.8 to 0.9 and therefore associated with the highly quenched monomer decay time), when collected at 500 nm, the preexponential factor associated with the longer component increases at the expense of the shorter component, which indicates the longer component to be associated with the

dx.doi.org/10.1021/ic301365y | Inorg. Chem. 2013, 52, 121−129

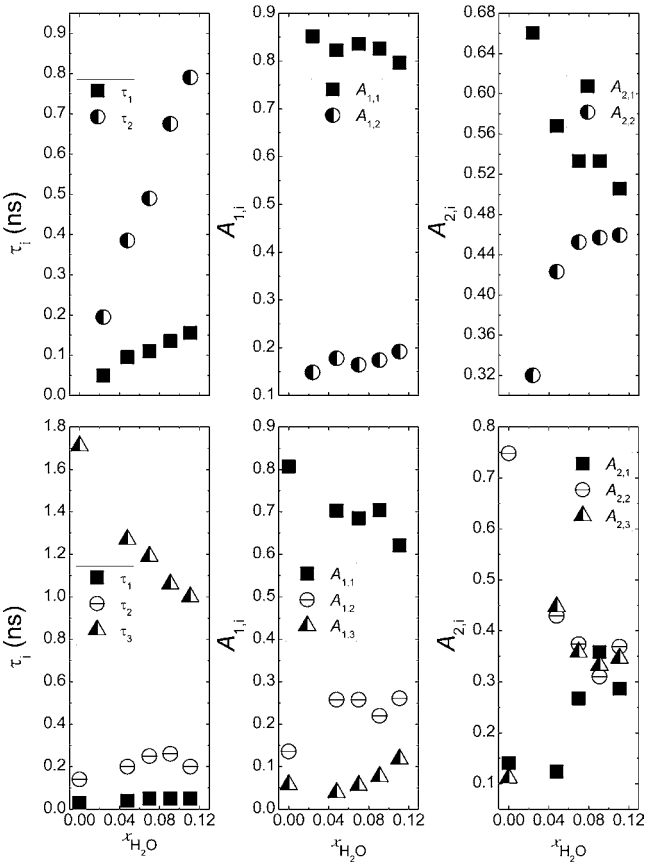

Figure 6. From left to right: Dependence of the decay times (τ_i) and preexponential factors obtained from the fluorescence decays collected at the monomer emission wavelength (420 nm, $A_{1,i}$) and at 500 nm for **P** and 550 nm for **L** ($A_{2,i}$) in dioxane/water mixtures (here expressed in mole fraction of water, x_{H_2O}). **P**: top panels. **L**: bottom panels.

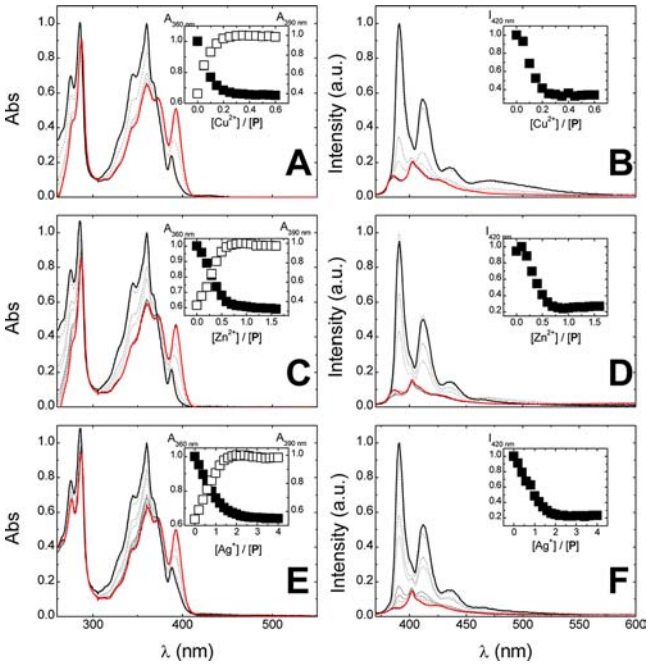

Figure 7. Absorption (left panels) and fluorescence emission (right panels) titrations of chemosensor **P** as a function of the increasing amounts of (A and B) $Cu(BF_4)_2$, (C and D) $Zn(BF_4)_2$, and (E and F) $Ag(BF_4)$ in dioxane. The insets show the absorption at 360 and 390 nm and the fluorescence intensity at 420 nm. [**P**] = 5.00 × 10^{-6} M, and λ_{exc} = 360 nm. The bold dark line is for [Cu^{2+}]/[**P**] = [Zn^{2+}]/[**P**] = [Ag^+]/[**P**] = 0, whereas the bold red line is [Cu^{2+}]/[**P**] = 0.6, [Zn^{2+}]/[**P**] = 1.6, and [Ag^+]/[**P**] = 4, respectively.

exciplex formed species. Furthermore, the reduced contribution of the longer decay time (preexponential factors varying from 0.1 to 0.2) mirrors the fact that the exciplex is also emitting at this emission wavelength. At 500 nm, the preexponential factor associated with the exciplex is dominant and increases with the water amount, in agreement with the steady-state spectra.

In the case of compound **L**, we now observed three decay times in which besides the two previously indicated τ_1 and τ_2, an additional longer decay time (with a value of ∼1 ns) is present but only with a significant contribution at longer emission wavelengths. In addition, the absence of a rising component at this emission wavelength gives a clear indication that the majority of this species is already present in the ground state.

Interaction of P and L with Metal Cations. In order to further explore the behavior of compounds **P** and **L** as potential chemosensors toward Cu^{2+}, Zn^{2+}, and Ag^+, additional studies involving titrations with these metal ions were performed.

The addition of incremental amounts of the metal cations to a dioxane solution of **P** leads to a decrease in the absorption maxima with, however, the same shape in the spectra; see Figure 7. The same is valid for the emission spectrum, which shows that the decrease of the fluorescence intensity is likely due to a quenching process that involves metal-ligand interaction in the ground state. It is worth noting that the I_0/I ratio for the same [metal ion]/[**P**] ratio is 5 times higher with Cu^{2+} than it is with Ag^+ and Zn^{2+}; although further studies with other metals are needed, this suggests a peculiar selectivity of **P** toward Cu^{2+}.

It is relevant to point out that in the presence of metal cations, for both **P** and **L**, the emission band of the exciplex is absent.

Figure 8 depicts the absorption and emission spectra of **L** in dioxane and in the presence of increasing amounts of Cu^{2+} (A and B), Zn^{2+} (C and D), and Ag^+ (E and F). Upon the addition of metal cations, the long wavelength absorption tail becomes well-defined with an isoabsorptive wavelength (425 nm for Cu^{2+}, 430 nm for Zn^{2+}, and 410 nm for Ag^+), which indicates a ground-state equilibrium between the monomer and dimer species. In contrast with this behavior, in the emission spectra, the intensity of the band collected at the monomer region (390 nm) increases and that for the excimer/dimer decreases upon metal addition with well-defined crossing points in the titration curve (see insets in Figure 7). This shows that, upon the addition of the metal cation, the pyrene units in **L** split, and there is an increment of the monomer emission with a decrease of the excimer/dimer emission.

The formation of a 1:1 (metal/ligand) stoichiometry after titration of **L** with Cu^{2+}, Zn^{2+}, and Ag^+ was confirmed unambiguously by the Job's plot method.[24] The new low-energy bands (ca. 121 nm red shift) were responsible for the change of color, perceptible to the naked eye, which is shown in Figure 9. In dioxane, the color of the solution changes from yellow to dark red (Cu^{2+}), intense red orange (Zn^{2+}), and intense gold yellow (Ag^+) after the addition of 1 equiv of the appropriate metal ion to a solution of **L** in the same solvent.

In the case of probe **P**, the color of the dioxane solution changes from pale yellow to intense yellow (Cu^{2+} and Zn^{2+})

dx.doi.org/10.1021/ic301365y | *Inorg. Chem.* 2013, 52, 121−129

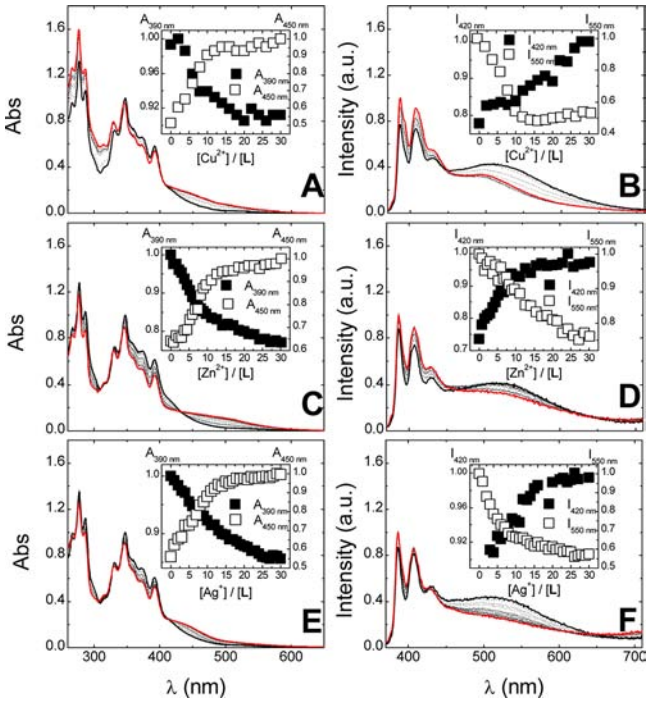

Figure 8. Absorption (left panels) and fluorescence emission (right panels) titrations of chemosensor **L** as a function of the increasing amounts of (A and B) $Cu(BF_4)_2$, (C and D) $Zn(BF_4)_2$, and (E and F) $Ag(BF_4)$ in dioxane. The insets show the absorption at 360 and 390 nm and the fluorescence intensity at 420 nm ($[\mathbf{L}] = 5.00 \times 10^{-6}$ M, and $\lambda_{exc} = 360$ nm). The bold dark line is for $[Cu^{2+}]/[\mathbf{L}] = [Zn^{2+}]/[\mathbf{L}] = [Ag^{+}]/[\mathbf{L}] = 0$, whereas the bold red line is for $[Cu^{2+}]/[\mathbf{L}] = [Zn^{2+}]/[\mathbf{L}] = [Ag^{+}]/[\mathbf{L}] = 30$.

and colorless (Ag^+) after the addition of 1 equiv of the appropriate metal ion.

From Figure 9, it can be seen that the colors observed in all cases are the result of the metal-to-ligand interaction and not just to the mixture of two (colored) solutions; e.g., in the case of Cu^{2+} when the (pale) blue solution of Cu^{2+} is added to the yellow solution of **L**, it should be green with just the result of color overlap and not dark red, as was obtained. These results suggest the use of **L** for colorimetric detection of the explored metal ions.

The stability constants for the interaction of **L** with Cu^{2+}, Zn^{2+}, and Ag^+ were calculated using *HypSpec* software and are summarized in Table 2.[25] Taking into account the values obtained, the strongest interaction expected for sensor **L** is with

Table 2. Stability Constants for Chemosensor L in the Presence of Cu^{2+}, Zn^{2+}, and Ag^+ in Dioxane for an Interaction 1:1 (Metal/Ligand)

compound	interaction (M/L) in dioxane	$\sum \log \beta$(absorption)	$\sum \log \beta$(emission)
L	Cu^{2+} (1:1)	$3.67 \pm 2.59 \times 10^{-3}$	$3.10 \pm 3.13 \times 10^{-2}$
	Zn^{2+} (1:1)	$3.99 \pm 1.81 \times 10^{-3}$	$4.08 \pm 8.01 \times 10^{-3}$
	Ag^+ (1:1)	$10.69 \pm 1.68 \times 10^{-3}$	$10.82 \pm 1.50 \times 10^{-2}$

Ag^+. These values are in agreement with the MALDI-TOF-MS results previously discussed.

In the case of **P**, we were unable to obtain with *HypSpec* the stability constants for the interaction with Ag^+, Cu^{2+}, and Zn^{2+}. In this case (**P**), a great number of equivalents of each metal ion were necessary to achieve a plateau (equilibrium). This result suggested **L** as the more favorable system over **P** for interaction with the explored metal ions. This could be due to the fact that a better stabilization of each metal ion was obtained with the bischromophoric system **L**.

Interaction between L and Metal Cations: Time-Resolved Data. Time-resolved data provide further and relevant information regarding the excimer-forming processes in the absence and presence of metal cations. In pure dioxane, the results presented so far have shown that the band at 390 nm can be attributed to a monomer emission, i.e., to an excited pyrene with no other pyrene in its vicinity. In the case of **L**, the longer emission wavelength can be attributed to the emission of an excimer/dimer. In order to avoid contribution/"contamination" of the monomer emission in the excimer region (and vice versa), we collected the emission decays in the extremities of each emission band: 420 nm (monomer) and 550 nm (excimer).

It is worth remembering that, from steady-state data, the exciplex emission is absent for **L** in the presence of metal cations. It is also worth noting the extraordinary quenching suffered by the decay times of these pyrene derivatives in comparison with other known and investigated pyrene system derivatives, i.e., from nano-[26] to picosecond (in our work with **P** and **L**) time regime. This shows that the imine groups are strong quenchers of pyrene fluorescence.

Figure 10 depicts the emission decays in dioxane in the absence (A) and presence (B) of Ag^+. Global analysis of the decays shows that these are again fitted with the sums of three exponentials. It is also worth noting that the decay times are generally kept constant upon the addition of Ag^+. However, the same does not happen with the preexponential factors.

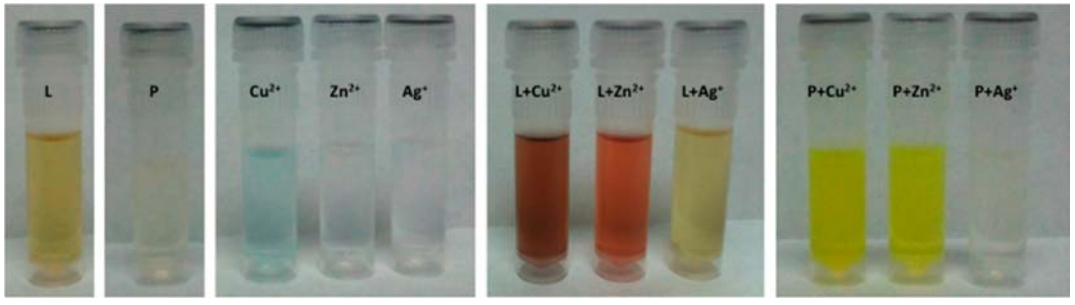

Figure 9. Color changes observed after the interaction of **L** (6.80×10^{-4} M) and **P** (1.00×10^{-4} M) with Cu^{2+} (1 equiv), Zn^{2+} (1 equiv), and Ag^+ (1 equiv) in dioxane. Initial colors of **L**, **P**, and metallic solutions.

dx.doi.org/10.1021/ic301365y | *Inorg. Chem.* 2013, 52, 121−129

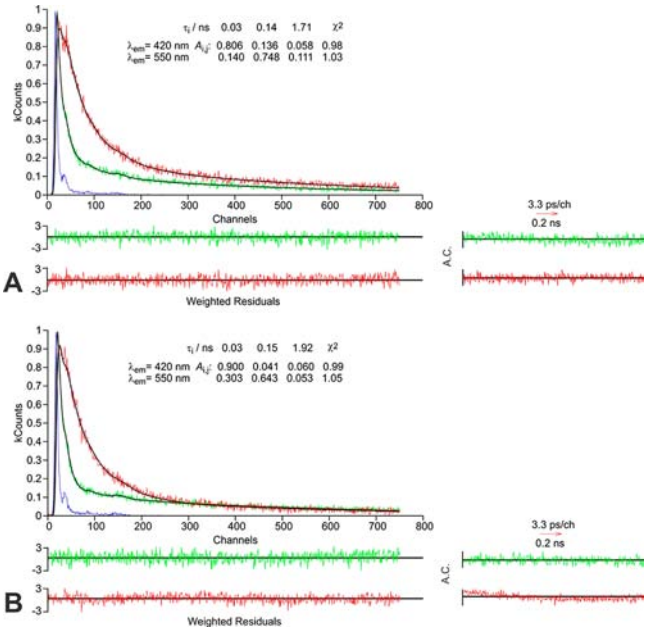

Figure 10. Fluorescence decays of **L** in dioxane (T = 293 K) at λ_{exc} = 381 nm in (A) absence and (B) presence of Ag^+ (ratio $[Ag^+]/[\mathbf{L}]$ = 2:1). The instrument profile curve, decay times (τ_i), preexponential factors ($A_{i,j}$), χ^2 values, weighted residuals, and autocorrelation functions (A.C.) are shown as the insets.

From Figure 10, it can be seen that, upon the addition of Ag^+ at λ_{em} = 420 nm, there is basically no change in the preexponential value associated with the shorter component (the decay associated with the monomer ~30 ps). However, the same is not valid with the $A_{2,1}$ preexponential at λ_{em} = 550 nm, where an increase is observed upon the addition of Ag^+. Indeed, the addition of Ag^+ leads to an increase (basically doubling the values) of the $A_{2,1}$ and $A_{2,3}$ preexponential factors, which means that upon complex formation the monomer contribution (at the excimer/dimer emission) increases and the excimer/dimer emission decreases as a result of complexation with the imine moieties and a consequent split of the pyrene chromophores.

In addition, it can also be seen that a substantial decrease occurs, upon the addition of Ag^+, with the preexponential factor associated with the 140−150 ps decay time (related to the decay of the excimer/dimer species) at λ_{em} = 420 nm. This means that the addition of Ag^+ leads to a decrease in the excimer-to-monomer reversibility.

With these facts in mind and also with the previous knowledge in polymer systems bearing pyrene pendant chromophores where the process of dimer formation has been shown to occur with tens of picoseconds,[27] we propose the following interpretation. The shorter decay component (~30 ps) should be attributed to the monomer decay that gives rise to the excimer/dimer. This is the major component at 420 nm with a preexponential factor (concentration of the species at time zero) of ~0.8−0.9 in both the absence and presence of Ag^+. This short component is kinetically linked to the ~0.14 ns component (which is associated with the decay of the instantaneously formed dimer/excimer). This is likely to be kinetically linked to the other species (the other long component with ~1.7−1.9 ns), which should be associated with the emission of a relaxed dimer.[25] This mirrors the quick rearrangement of the pyrene groups in the (instantaneously formed) dimer to a more stable (dimer) conformation.

CONCLUSIONS

In this work, the synthesis and characterization of two new compounds, **P** and **L**, containing pyrene units was undertaken. The investigation of these two chemosensors has shown that these are sensitive to water and metal cations. In the case of water sensing, the two ligands showed a new band that was attributed to an exciplex species and whose contribution increases with the water amount. The interaction of **L** toward Cu^{2+}, Zn^{2+}, Ag^+, Cd^{2+}, and Hg^{2+} metal ions was also explored in the gas phase using MALDI-TOF-MS.

Several metal-ion titrations of **L** with Cu^{2+}, Ag^+, and Zn^{2+} followed by absorption and emission studies were performed in dioxane. In all cases, the stability constant values suggest a stoichiometry of 1:1 ligand/metal. The strongest interaction expected for sensor **L** was with Ag^+ in all of the solvents tested, with the highest value being observed in the noncoordinative solvent dioxane. Compound **P** was found to be more selective to Cu^{2+}.

Further detailed information could be obtained from time-resolved experiments: (1) Extraordinary quenching is suffered by these pyrene derivatives, mirrored from the decrease from nanoseconds, the usual range of pyrene derivative lifetimes, to picoseconds, which is likely due to the imine groups that are strong quenchers of pyrene fluorescence. (2) Global analysis of the emission decays in dioxane in the absence and presence of Ag^+ shows that the decays are only fitted with the sums of three exponentials, which were associated with the monomer, and the two additional components with the kinetics of a dimer formation.

ASSOCIATED CONTENT

Supporting Information

Synthetic details, excitation spectra of **P** and **L** with the addition of metals (Cu^{2+}, Zn^{2+}, and Ag^+) and water collected at λ_{em} = 420 and 500 nm, and absorption and emission spectra of **L** in pure dioxane before and after the removal of water. This material is available free of charge via the Internet at http://pubs.acs.org.

AUTHOR INFORMATION

Corresponding Author

*E-mail: sseixas@ci.uc.pt (J.S.S.d.M.), clodeiro@uvigo.es or cle@fct.unl.pt (C.L.). Tel: +351 212948300 (C.L.). Fax: +34 988 387001 or +351 212948550 (C.L.).

Notes

The authors declare no competing financial interest.

ACKNOWLEDGMENTS

We are grateful to Xunta de Galicia (Spain) for Project 10CSA383009PR (Biomedicine) and to the Scientific Association Proteomass for financial support. J.F.-L. thanks Xunta de Galicia (Spain) for a research contract by Project 09CSA043383PR in Biomedicine. C.N. and C.S.d.C. thanks the Fundação para a Ciência e a Tecnologia/FEDER (Portugal/EU) programme postdoctoral Contracts SFRH/BPD/65367/2009 and SFRH/BD/75134/2010, respectively. J.L.C. and C.L. thank Xunta de Galicia for the Isidro Parga Pondal Research program. E.B. thanks the CCCU Research Development and Enhancement Fund.

REFERENCES

(1) (a) Liu, D. W.; Wang, Z.; Jiang, X. *Nanoscale* **2011**, *3*, 1421. (b) Manandhar, E.; Wallace, K. J. *Inorg. Chim. Acta* **2012**, *381*, 15.

(2) (a) Linton, B.; Hamilton, A. D. *Chem. Rev.* **1997**, *97*, 1669. (b) Godman, M. S.; Weiss, J.; Hamilton, A. D.; Jubian, V.; Linton, B.; Hamilton, A. D. *J. Am. Chem. Soc.* **1995**, *117*, 11610. (c) Al-Sayah, M.; Branda, N. R. *Angew. Chem., Int. Ed.* **2000**, *39*, 945. (d) Moriuchi, T.; Nishiyama, M.; Hirao, T. *Eur. J. Inorg. Chem.* **2002**, 447. (e) Jiao, T. F.; Liu, M. H. *J. Phys. Chem. B* **2005**, *109*, 2532. (f) Ramstrom, O.; Lehn, J. M. *Nat. Rev. Drug Discovery* **2002**, *1*, 26.

(3) Ma, Z.; Yang, R. D.; Yan, L. *J. Chem. Res., Synop.* **1999**, *12*, 712.

(4) (a) Radecka-Paryzek, W.; Patroniak, V.; Lisowski, J. *Coord. Chem. Rev.* **2005**, *249*, 2156. (b) Herrera, A. M.; Kalayda, G. V.; Disch, J. S.; Wilstrom, R. P.; Korendovych, I. V.; Staples, R. J.; Campana, C. F.; Nazarenko, Q. Y.; Haas, T. E.; Rybak-Akimova, E. V. *Dalton Trans.* **2003**, *23*, 4482. (c) Menon, S. C.; Panda, A.; Singh, H. B.; Butcher, R. J. *Chem. Commun.* **2000**, *2*, 143.

(5) (a) Chaviara, A. T.; Cox, P. J.; Repana, K. H.; Pantazaki, A. A.; Papazisis, K. t.; Kortsaris, A. H.; Kyriakidis, D. A.; St. Nikolov, G.; Bolos, C. A. *J. Inorg. Biochem.* **2005**, *99*, 467. (b) Won, D. H.; Lee, C. H. *Tetrahedron Lett.* **2001**, *42*, 1969. (c) Adams, H.; Elsegood, M. R. J.; Fenton, D. E.; Heath, S. L.; Ryan, S. J. *Inorg. Chem. Commun.* **1999**, *2*, 139. (d) Adams, H.; Fenton, D. E.; Ryan, S. J. *Inorg. Chem. Commun.* **1999**, *2*, 52. (e) Adams, H.; Bailey, N. A.; Collinson, S. R.; Fenton, D. E.; Hawley, J. C.; Kitchen, S. J. *J. Organomet. Chem.* **1998**, *550* (8), 7. (f) Dias, P.; Domenech, A.; García-España, E.; Soriano, C. *Polyhedron* **2002**, *21*, 1523.

(6) (a) Lodeiro, C.; Capelo, J. L.; Mejuto, J. C.; Oliveira, E.; Santos, H. M.; Pedras, B.; Núñez, C. *Chem. Soc. Rev.* **2010**, *39*, 2948. (b) Lodeiro, C.; Pina, F. *Coord. Chem. Rev.* **2009**, *253*, 1353. (c) Núñez, C.; Bastida, R.; Macías, A.; Valencia, L.; Neuman, N. I.; Rizzi, A. C.; Brondino, C. D.; González, P. J.; Capelo, J. L.; Lodeiro, C. *Dalton Trans.* **2010**, *39*, 11654. (d) Núñez, C.; Bastida, R.; Macías, A.; Valencia, L.; Ribas, J.; Capelo, J. L.; Lodeiro, C. *Dalton Trans.* **2010**, *39*, 7673.

(7) (a) Jiang, P. G.; Chen, L. Z.; Lin, J.; Liu, Q.; Ding, J.; Gao, X.; Guo, Z. *Chem. Commun.* **2002**, 1424. (b) Zhang, H.; Han, L.-F.; Zachariasse, K. A.; Jiang, Y. B. *Org. Lett.* **2005**, *7*, 4217. (c) He, Q.; Miller, E. W.; Wong, A. P.; Chang, C. J. *J. Am. Chem. Soc.* **2006**, *128*, 9316. (d) Martínez, R.; Zapata, F.; Caballero, A.; Espinosa, A.; Tairraga, A.; Molina, P. *Org. Lett.* **2006**, *8*, 3235. (e) Avirah, R. R.; Jyothish, K.; Ramaiah, D. *Org. Lett.* **2007**, *9*, 121. (f) Yoon, S.; Miller, E. W.; He, Q.; Do, P. H.; Chang, C. J. *Angew. Chem., Int. Ed.* **2007**, *46*, 6658. (g) Shiraishi, Y.; Maehara, H.; Ishizumi, K.; Hirai, T. *Org. Lett.* **2007**, *9*, 3125. (h) Mameli, M.; Lippollis, V.; Caltagirone, C.; Capelo, J. L.; Nieto-Faza, O.; Lodeiro, C. *Inorg. Chem.* **2010**, *49*, 8276. (i) Oliveira, E.; Baptista, R. M. F.; Costa, S. P. G.; Raposo, M. M. M.; Lodeiro, C. *Inorg. Chem.* **2010**, *49*, 10847.

(8) (a) Prodi, L.; Bolletta, F.; Montalti, M.; Zaccheroni, N. *Coord. Chem. Rev.* **2000**, *205*, 59. (b) de Silva, A. P.; Gunaratne, H. Q. N.; Gunnlaugsson, T.; Huxley, A. J. M.; McCoy, C. P.; Rademacher, J. T.; Rice, T. E. *Chem. Rev.* **1997**, *97*, 1515. (c) Fabbrizzi, L.; Poggi, A. *Chem. Soc. Rev.* **1995**, *24*, 197. (d) Valeur, B.; Leray, I. *Coord. Chem. Rev.* **2000**, *205*, 3.

(9) (a) Czarnik, A. W. *Acc. Chem. Res.* **1994**, *27*, 302. (b) de Silva, A. P.; Gunaratne, H. Q. N.; Gunnlaugsson, T. A.; Huxley, T. M.; McCoy, C. P.; Rademacher, J. T.; Rice, T. E. *Chem. Rev.* **1997**, *97*, 1515. (c) Gunnlaugsson, T.; Glynn, M.; Tocci, G. M.; Kruger, P. E.; Pfeffer, F. M. *Coord. Chem. Rev.* **2006**, *250*, 3094. (d) Kim, J. S.; Quang, D. T. *Chem. Rev.* **2007**, *107*, 3780. (e) Xu, Z.; Chen, X.; Kim, H. N.; Yoon, J. *Chem. Soc. Rev.* **2010**, *39*, 127. (f) Chen, X.; Zhou, Y.; Peng, X.; Yoon, J. *Chem. Soc. Rev.* **2010**, *39*, 2120. (g) Xu, Z.; Kim, S. K.; Yoon, J. *Chem. Soc. Rev.* **2010**, *39*, 1457. (h) Kim, H. N.; Guo, Z.; Zhu, W.; Yoon, J.; Tian, H. *Chem. Soc. Rev.* **2011**, *40*, 79. (i) Chen, X.; Kang, S.; Kim, M. J.; Kim, J.; Kim, Y. S.; Kim, H.; Chi, B.; Kim, S.-J.; Lee, J. Y.; Yoon, J. *Angew. Chem., Int. Ed.* **2010**, *49*, 1422. (j) Xu, Z.; Baek, K.-H.; Kim, H. N.; Cui, J.; Qian, X.; Spring, D. R.; Shin, I.; Yoon, J. *J. Am. Chem. Soc.* **2010**, *132*, 601.

(10) Kim, J. S.; Quang, D. T. *Chem. Rev.* **2007**, *107*, 3780.

(11) Valeur, B. *Molecular Fluorescence Principles and Applications*; Wiley-VCH: New York, 2002.

(12) (a) Winnik, F. M. *Chem. Rev.* **1993**, *93*, 587. (b) Nishizawa, S.; Kato, A.; Teramae, N. *J. Am. Chem. Soc.* **1999**, *121*, 9463. (c) Sahoo, D.; Narayanaswami, V.; Kay, C. M.; Ryan, R. O. *Biochemistry* **2000**, *39*, 6595. (d) Kim, S. K.; Yoon, J. *J. Org. Chem.* **2003**, *68*, 597. (e) Yuasa, H.; Miyagawa, N.; Izumi, T.; Nakatani, M.; Izumi, M.; Hashimoto, H. *Org. Lett.* **2004**, *6*, 1489.

(13) (a) Zachariasse, K. A.; Duveneck, G.; Kuhnle, W. *Chem. Phys. Lett.* **1985**, *113*, 337. (b) Seixas de Melo, J.; Costa, T.; Francisco, A.; Maçanita, A. L.; Gago, S.; Gonçalves, I. S. *Phys. Chem. Chem. Phys.* **2007**, *9*, 1370.

(14) (a) Shiraishi, Y.; Tokitoh, Y.; Hirai, T. *Org. Lett.* **2006**, *8*, 3841. (b) Kim, H.; Hong, J.; Hong, A.; Ham, S.; Lee, J.; Kim, J. S. *Org. Lett.* **2008**, *10*, 1963. (c) Jung, H.; Park, M.; Han, D.; Kim, E.; Lee, C.; Ham, S.; Kim, J. S. *Org. Lett.* **2009**, *11*, 3378.

(15) (a) Moon, S. Y.; Youn, N. J.; Park, S. M.; Chang, S. K. *J. Org. Chem.* **2005**, *70*, 2394. (b) Kim, J. S.; Choi, M. G.; Song, K. C.; No, K. T.; Ahn, S.; Chang, S. K. *Org. Lett.* **2007**, *9*, 1129. (c) Park, S. M.; Kim, M. H.; Choe, J. I.; No, K. T.; Chang, S. K. *J. Org. Chem.* **2007**, *72*, 3550. (d) Xu, Z.; Yoon, J.; Spring, D. R. *Chem. Commun.* **2010**, *46*, 2563.

(16) (a) Xie, J.; Menand, M.; Maisonneuve, S.; Metivier, R. *J. Org. Chem.* **2007**, *72*, 5980. (b) Zhang, H.; Han, L. F.; Zachariasse, K. A.; Jiang, Y. B. *Org. Lett.* **2005**, *7*, 4217. (c) Yang, J. S.; Lin, C. S.; Hwang, C. Y. *Org. Lett.* **2001**, *3*, 889. (d) Hung, H. C.; Cheng, C. W.; Ho, I. T.; Chung, W. S. *Tetrahedron Lett.* **2009**, *50*, 302. (e) Hung, H.-C.; Cheng, C.-W.; Wang, Y.-Y.; Chen, Y.-J.; Chung, W.-S. *Eur. J. Org. Chem.* **2009**, 6360.

(17) Pina, J.; Seixas de Melo, J. S.; Burrows, H. D.; Maçanita, A. L.; Galbrecht, F.; Bunnagel, T.; Scherf, U. *Macromolecules* **2009**, *42*, 1710.

(18) Striker, G.; Subramaniam, V.; Seidel, C. A. M.; Volkmer, A. *J. Phys. Chem. B* **1999**, *103*, 8612.

(19) (a) Vicente, M.; Lodeiro, C.; Adams, H.; Bastida, R.; de Blas, A.; Fenton, D. E.; Macías, A.; Rodríguez, A.; Rodríguez-Blas, T. *Eur. J. Inorg. Chem.* **2000**, *6*, 1015. (b) Lodeiro, C.; Bastida, R.; de Blas, A.; Fenton, D. E.; Macías, A.; Rodríguez, A.; Rodríguez-Blas, T. *Inorg. Chim. Acta* **1998**, *267*, 55.

(20) Fernández-Lodeiro, J.; Núñez, C.; Carreira, R.; Santos, H. M.; Silva López, C.; Mejuto, J. C.; Capelo, J. L.; Lodeiro, C. *Tetrahedron* **2011**, *67*, 326.

(21) Birks, J. B. *Photophysics of Aromatic Molecules*; Wiley: London, 1970.

(22) Åkerlöf, G. O.; Short, A. *J. Am. Chem. Soc.* **1936**, *58* (7), 1241–1243.

(23) Bichenkova, E. V.; Sardarian, A. R.; Wilton, A. N.; Bonnet, P.; Bryce, R. A.; Douglas, K. T. *Org. Biomol. Chem.* **2006**, *4*, 367.

(24) MacCarthy, P. *Anal. Chem.* **1978**, *50*, 2165.

(25) Gans, P.; Sabatini, A.; Vacca, A. *Talanta* **1996**, *43*, 1739.

(26) (a) Lodeiro, C.; Lima, J. C.; Parola, A. J.; Seixas de Melo, J. S.; Capelo, J. L.; Covelo, B.; Tamayo, A.; Pedras, B. *Sens. Actuators, B* **2006**, *115*, 276. (b) Seixas de Melo, J. S.; Costa, T.; Francisco, A.; Maçanita, A. L.; Gago, S.; Gonçalves, I. S. *Phys. Chem. Chem. Phys.* **2007**, *9*, 1370.

(27) Costa, T.; Seixas de Melo, J. S.; Castro, C. S.; Gago, S.; Pillinger, M.; Gonçalves, I. S. *J. Phys. Chem. B* **2010**, *114*, 12439.